

SeaWinds 1B: a combination of Ku-band scatterometer and wind radiometer for global ocean wind measurements

Wu-yang Tsai, James E. Graf, Carroll Winn, and Simon Yueh

Jet Propulsion Laboratory, California Institute of Technology,
4800 Oak Grove Drive, Pasadena, CA 91109

ABSTRACT

Satellite wind scatterometers are microwave radar instruments designed specifically to measure near-surface wind speed and direction over the global ocean. NASA has a long term commitment to ocean wind remote sensing, starting from Seasat-A Satellite Scatterometer (SASS), through NASA Scatterometer (NSCAT), to SeaWinds-1. SASS was launched in June, 1978 and operated for three months. NSCAT was launched on Japan's Advanced Earth Observation Satellite (ADEOS) in August, 1996, and SeaWinds-1 will be launched on ADEOS-2 in 1999. As a continuation of the NASA wind measurement program, we are developing a next generation wind vector measurement instrument called SeaWinds-1 B, scheduled to be launched in year 2003 on Japan's Advanced Earth Observation Satellite-3 (ADEOS-3). The purpose of this paper is to present the system parameters and system design of this new instrument.

SeaWinds-1B is a combination of three instruments into a single design: scatterometer, radiometer, and polarimetric wind-radiometer. The scatterometer instrument is used as a baseline to continue the active microwave wind measurements. The polarimetric wind-radiometer (WIN DRAD) instrument is incorporated to demonstrate a new concept of wind vector measurements from space using polarimetric radiometer. WIN DRAD can also be used to measure the atmospheric attenuation to improve the scatterometer measurement accuracy. Furthermore, the combination of the scatterometer and WIN DRAD will improve the accuracy of the wind vector measurements and the skills for removing the wind direction retrieval ambiguity. This instrument, if proven successfully, has the potential to become the next generation operational ocean remote sensing instrument.

Keywords: scatterometer, microwave, polarimetric radiometer, winds.

1. INTRODUCTION

Satellite wind scatterometers are microwave radar instruments designed specifically to measure near-surface wind speed and direction over the global ocean. NASA has a long term commitment to ocean wind remote sensing, starting from Seasat-A Satellite Scatterometer (SASS)¹, through NASA Scatterometer (NSCAT)², to SeaWinds-1. SASS was launched in June, 1978 and operated for three months. NSCAT was launched on Japan's Advanced Earth Observation Satellite (ADEOS) in August, 1996, and SeaWinds-1³ will be launched on ADEOS-2 in 1999. As a continuation of the NASA wind measurement program, we are developing a next generation wind vector measurement instrument, called SeaWinds-1B, planned to be launched in year 2003 on Japan's Advanced Earth Observation Satellite-3 (ADEOS-3).

SeaWinds-1B is a combination of three instruments into a single design: scatterometer, radiometer, and polarimetric wind-radiometer. The Ku-band scatterometer instrument is used as a baseline to continue the

active microwave wind measurements. This Ku-band scatterometer has the following unique features: (1) it uses a rotating parabolic dish with two circular scanning beams, (2) it is capable to obtain higher resolution sigma-O (2 km x 20 km) through the transmission of a linear frequency modulated chirp with a bandwidth of about 1.5 MHz, and (3) it will use a helix tube instead of TWTA to significantly reduce the mass and volume of the electronics system.

The polarimetric wind-radiometer (WINDRAD)⁴ instrument is incorporated to demonstrate a new concept of wind vector measurements from space using polarimetric radiometer (5). WINDRAD can also be used to measure the atmospheric attenuation to improve the scatterometer measurement accuracy. Furthermore, the combination of the scatterometer and WINDRAD will improve the accuracy of the wind vector measurements and the skills for removing the wind direction retrieval ambiguity. This instrument if proven successfully, has the potential to become the next generation operational ocean remote sensing instrument. The purpose of this paper is to present the conceptual design of this new instrument.

2. OBJECTIVES OF SEAWINDS1B MISSION

The primary objective of the SeaWinds 1B mission is to continue the active microwave wind measurements, as part of NASA's Mission of Planet Earth, to monitor the global ocean for studying the short and long term climate change of the Earth.

The secondary objective of this mission is to inject new technology and improvements to the SeaWinds 1A design for increasing reliability and reducing mass and power requirements, and to enhance the resolution and performance of the pencil beam scatterometer system. As will be described later in Section 3, this is accomplished by (1) using magnetic bearings, (2) moving RF subsystem to the spun side, (3) reducing system loss through design improvement, (4) using off-set feed-horns and larger antenna size, and (5) using helix tubes, higher chirp rate, and larger FFT size.

As an investment for the future, we are also incorporating a three-frequency polarimetric wind radiometer instrument in SeaWinds1B mission to demonstrate the feasibility of passive microwave radiometry for large spatial coverage of ocean surface wind vector measurements. This instrument, if proven successfully, has the potential to become the next generation operational ocean remote sensing instrument.

3. OVERVIEW OF THE SEAWINDS1B SYSTEM

SeaWinds 1 B is currently design to be accommodated by ADEOS-3, planned for launch in 2003. It is required to have five years mission. The nominal orbit is sun-synchronous with 98.6° inclination, with orbit altitude of 803 km, 4 days exact repeat.

Since ADEOS-3 is still in the drawing stage, the spacecraft configuration is still unclear at this point. As a demonstration of accommodation concept, a cartoon drawing of the SeaWinds 1B on board of the ADEOS-2 is shown in Figure 1. As shown in the figure, the scatterometer and polarimetric radiometer system shares a single compact high-performance dual-reflector antenna. This new antenna design will enable us to accommodate an array of off-set feed horns on a focal planes with up to 15° angular beam separation, while it meets the beam efficiency and sidelobe requirements. The antenna system is spinning, at a rate of 18 rpm about a nadir axis. The Ku-band scatterometer has two antenna beams: inner beam at 40° and outer beam at 46° look angles, while WINDRAD has three look angles: 38.9°, 45.2°, and 53.6°.

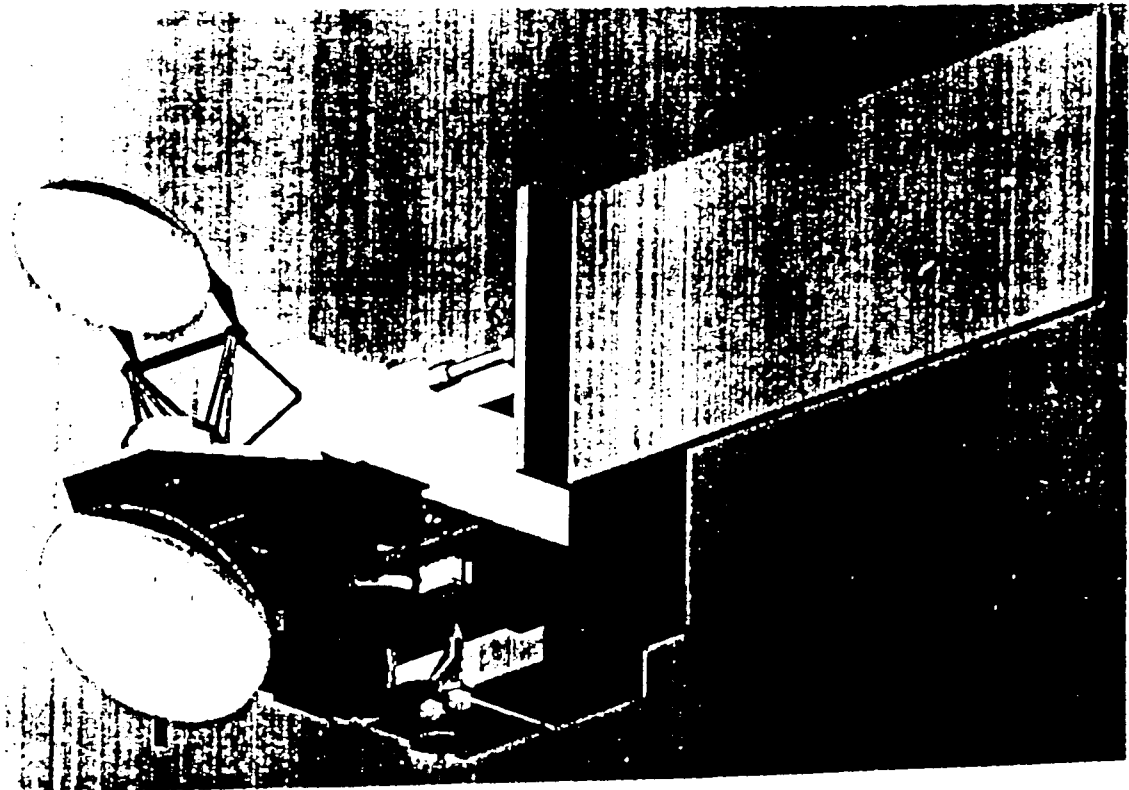
A list of the key system parameters for both the scatterometer and WINDRAD is shown in Table 1.

An overall system functional block diagram is shown in Figure 2. As shown in the figure, all scatterometer and WINDRAD RF electronics are located on the spun side to minimize the system loss and to increase the reliability and stability of the system (without using rotary joint).

Table 1. Key SeaWinds 1 B System Parameter

ScatterometerSystem:	
Look angles	40° and 46°
Swath radius (km)	705 km (inner), 900 km (outer)
Transmit frequency	13.402 ± 0.005 Ghz
Pulse width	2.65 ms (inner), 1.55 ms (outer)
Pulse Repetition Frequency	190 Hz
Antenna I-way 3 dB beamwidth	1.19° (azimuth), 1.40° (elevation)
2-way 3dB footprint (km)	16.1 (az) x 27.5 (cl) inner
	18.2 (az) x 36.6 (cl) outer
Antenna Gain (for Ku-band)	42 dB
Polarization	H (inner), V (outer)
Distance between pulses	14.4 km (inner), 18.3 km (outer)
Chirp rate	1.0 Mhz/ms
Dechirp Bandwidth	210 kHz (inner), 280 kHz (outer)
Resolution per slice	2 km x 20 km
Data rate	142 kbps
WINDRADSystem:	
Look angles	38.9°, 45.2°, 53.6°
Frequency (Ghz)	18, 22, 37
Polarization	Tv, Th, U and V for 18 and 37 Ghz
	Tv and Th for 22 GHz
Swath width (km)	1360, 1700, 2500
Radiometer sensitivity per footprint	0.1° K
Radiometer calibration stability	0.1° K
Radiometer absolute calibration accuracy	2° K
Datarate	45 kbps

Figure 1. Artist Conception of SeaWinds 1 B on ADEOS-2



4. SEAWINDS 1B SCATTEROMETER SYSTEM

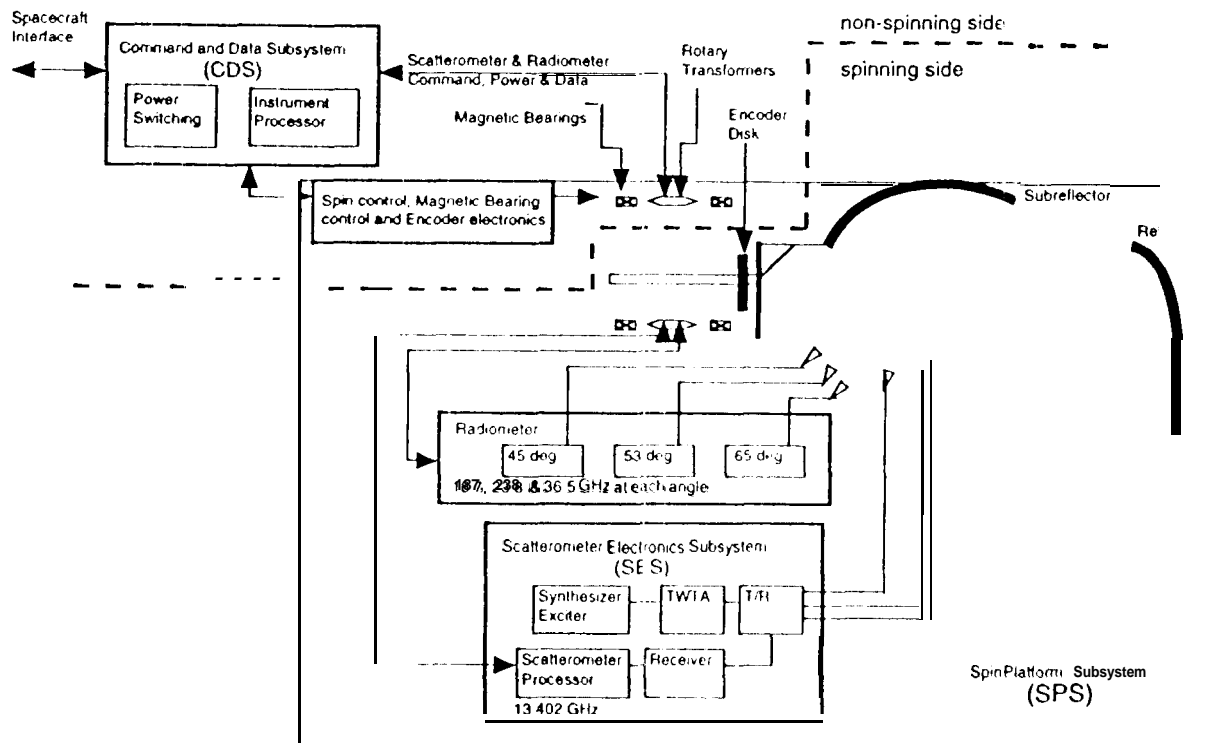
4.1 Background

Wind scatterometers are radars specifically designed to measure **wind velocities over the oceans**. Microwave scatterometer measurements **have been shown to be sensitive to ocean surface winds in a number of airborne campaigns**, the Skylab S-193 RADSCAT and SeaSat Scatterometer (SASS) experiments. Following the SASS experiment, the **ERS⁵** series of satellites with on board C-band microwave scatterometers has **been** in operation since 1991. The NASA Scatterometer (**NSCAT**) on board of the Japanese Advanced Earth Observation Satellite (**ADEOS**) was launched on August 17, 1996 has been operated successfully. **Its** wide swath and high quality winds have been found to have to **have a** significant impact on numerical **weather** forecasting, storm monitoring and many other scientific applications. Follow on NASA and ESA satellite scatterometers have been planned to extend the time series of satellite wind products to the 21st century.

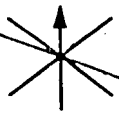
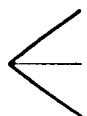
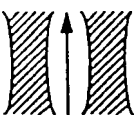
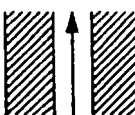
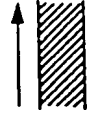
Scatterometers can measure **ocean surface winds** because the dependence of radar **backscatter (σ_0)** on **ocean surface roughness**, which is a function of surface wind velocity. Changes in wind **velocity** cause changes in the roughness of these surface waves. Directional response of the ocean surface to wind forcing makes the profiles of gravity and capillary waves rougher in the along-wind direction than those across. The surface waves and foam interact with **radar** waves and the strength of the returned echoes provide a **link** between backscatter and surface wind **speed** and direction.

Since σ_0 depends on both wind speed and direction, a single σ_0 measurement is inadequate for retrieval of both variables. To retrieve the wind vector, multiple measurements are made at several different azimuth angles. Fig. 3 depicts the measurement geometry of SASS, ERS, NSCAT, and SeaWinds scatterometers. SASS collected measurements at two azimuth angles separated by 90 degrees, and there are up to four possible wind directions for the SASS measurement geometry. To reduce the number of wind direction solutions (ambiguities), NSCAT **added** two mid-antenna beams to the SASS antenna geometry. Another improvement of NSCAT over SASS is the use of on-board digital Doppler filtering. This enables us to sharpen the broad fan beams into finer resolutions. The baseline resolution is 25 km cross track.

Figure 2. SeaWinds 1B Functional Block Diagram



**Figure 3. Comparison of Spaceborne Scatterometers
Past, Present, and Future**

	SASS	NSCAT	SeaWinds	ERS-1/2
Frequency	14.6 GHz	13.993 GHz	13.402 GHz	5.3 GHz
Scan Pattern				
Polarization	V-H, V-H	V, V-H, V	V, H	V ONLY
Beam Resolution	Fixed Doppler	Variable Doppler	Spot	RANGE GATE
Resolution	50/100 km	25/50 km	35/50 km	25/50 km
Swath				
Daily / 2-day Coverage	Variable	77/97%	9W/100%	41%
Dates	6/78 - 10/78	8/96 - 8/99	2/99 - 2/02	01 +

SeaWinds² is the follow-on to NSCAT. It is scheduled to launch on November, 1999 for a three year mission. SeaWinds also operated at Ku-band. SeaWinds system represents a major design change of NASA scatterometers. Instead of using the fan beam design, SeaWinds will use a conical scanning reflector. This is due to the accommodation requirement by ADEOS-2, which can not provide a clear field-of-view for NSCAT-like fan beam antennas with broad elevation antenna beam patterns. The SeaWinds reflector is illuminated by two offset center-fed antenna feedhorns, resulting in two spot beams illuminating the earth surface at 46.3° and 54.1° incidence angles. The outer beam operates at vertical polarization and the inner beam at horizontal polarization. Because the horizontally polarized ocean backscatter has a larger upwind-downwind asymmetry than the vertically polarized response, the mixed polarization combination was determined to have a better ambiguity selection skill than the other combinations. The antenna reflector is mounted on a spinning assembly with a nominal rotation rate of 18 rpm. The antenna footprints produced by these two antenna beams will trace out two circles on the earth surface, enabling two to four azimuth radar observations for a given spot on the earth surface. The relative azimuth angles of these observations vary across the swath, unlike the fan beam designs where the relative azimuth angles are essentially constant from near to far swath. The varying azimuth geometry degrades the measurement performance at outer swath and near nadir track where the azimuth angles between the fore and aft looks reduces to zero or 180 degrees.

Because of the change of antenna design, the signal detection principle and hence the electronics design of SeaWinds is also different from those of NSCAT. The resolution of the SeaWinds radar footprints is basically defined by the size of antenna reflector (two-ways) and is about 37km in range and 26 km in azimuth for the outer beam. To improve the range resolution, the SeaWinds RF electronics can be commanded to transmit a chirp signal at 250 Mhz/ms in one pulse length of 1.5 ms. On-board digital processing will then apply range compression to divide the radar echo into six range cells, resulting in about 7 km resolution in range. This makes the size of SeaWinds measurement cell comparable to the nominal resolution cell of NSCAT (except reversing the range and azimuth resolution)

Another improvement feature of the SeaWinds scanning geometry is that the measurement swath is contiguous without a gap near the subsatellite nadir track, which is present in fan-beam scatterometer designs. Although the accuracy of retrieved wind velocity near the spacecraft nadir track is not as good as

that in the mid-swath, a contiguous swath does allow SeaWinds to image 90% of global ice-free oceans in one day compared to about 78% for NSCAT.

4.2 SeaWinds 1B Scatterometer Electronic Subsystem Design

The design philosophy of the SeaWinds 1B electronic subsystem (SES-1B) is to inherit the SeaWinds 1A (SES-1A) design as much as possible. The key differences between the SES-1A and SES-1B is summarized in Table 2. A study on modifying SES-1A hardware to meet SES-1B requirement was conducted by Raytheon E-Systems.

Figure 4 shows the block diagram of the SES-1B electronics subsystem. The exciter generates first and second LO frequencies at 775 MHz and 12.627 GHz phase-locked to the 28.375 MHz STALO. The frequency synthesizer outputs a linear frequency modulated chirp signal at 1 MHz/ms centered at 775 MHz. The IF signal is then mixed up to 13.402 GHz, amplified by a helix tube, and sent through the T/R switch to the Scatterometer Antenna Subsystem (SAS). On receive, the echo is pre-amplified by an LNA located immediately after the T/R switch, mixed down to IF, and I/Q demodulated to baseband video signal.

The Scatterometer Controller and Processor (SCP) has two main functions: (a) it controls the system timing, pulse repetition frequency, and frequency synthesis parameters, and (b) it de-chirps the echo signal, performs FFT and bins the periodogram into 128 range cells. The general-purpose digital signal processor (DSP) in SCP also serves as the interface to the Command and Data Subsystems (CDS) to transfer commands and data.

A major change from the SES-1A is the increased chirp rate which not only improves the signal-to-noise ratio, but also allows better range discrimination. The pulse widths for both inner and outer beams are increased to give a further $B\tau$ improvement over that of the SES-1A. Since SeaWinds uses pencil-beam antennas with limited number of independent samples for each σ_0 measurement, the pulse widths are designed such that virtually no gap exists between transmit and receive cycles.

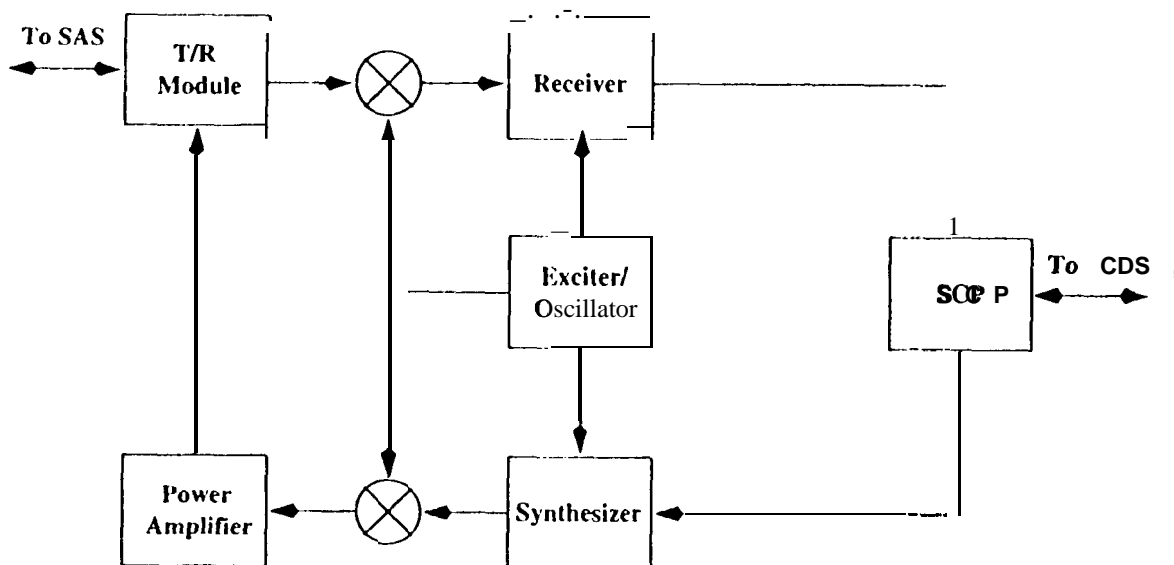
A further improvement over SW-1A is the movement of the RF electronics to the spinning side of the platform. This modification eliminates the need for RF rotary joints which are lossy and are subject to wear and tear over mission life. The low-noise-amplifier is also moved from the receiver to the output port of the T/R switch to improve the system noise figure.

To accommodate the increased bandwidth, the I/Q video signal has to be sampled at a much higher rate -- up to 5MS/sec for chirped echo if de-chirping is to be performed in DSP. An optional approach is to use a RF de-chirping scheme where the echo is de-chirped at IF before I/Q demodulated. This will reduce the Nyquist sample rate significantly and buys more processing time. This approach is currently under study.

Table 2. Key Differences between SES-1A and SES-1B

	SES-1A	SES-1B
Pulse width and PRF	1.5 ms (inner) 1.5 ms (outer) 185 Hz PRF	2.65 ms (inner) 1.55 ms (outer) 190 Hz PRF
Chirp rate	250 kHz/ms	1.0 MHz/ms
FFT size	7 km resolution bins in 6 cells	1 km resolution bins in 128 cells
Mounting of RF electronics	fixed on stationary platform, separated from antenna subsystem	on the spinning platform (integrated with antenna subsystem)

Figure 4. SeaWinds 1B electronics subsystem functional block diagram



5. SEAWINDS 1B WINDRAD SYSTEM

5.1 Background

The sensitivity of sea surface brightness temperatures to ocean wind speed has been demonstrated in many early studies and has' been applied to global measurements of ocean surface wind speed using spaceborne **radiometers**, such as the Scanning Multichannel Microwave Radiometer (SMMR) flown on NIMBUS-7 and SEASAT and the Special Sensor Microwave/Imager (SSM/I) deployed on the Defense Meteorological Satellite Program (DMSP) missions',

Recent experimental and theoretical studies have shown that there are wind direction signals in sea surface brightness temperatures. The airborne radiometer **measurements** acquired by Russian scientists at the Space Research Institute (SRI) measured sea surface brightness temperatures in 1980's indicated that the vertically and horizontally polarized microwave radiation from sea surfaces vary with the wind direction at near normal incidence angles^{7,8}. The analysis of SSM/I 19 and 37 GHz data by Wentz⁹ has revealed a few Kelvin directional signals in both T_v and T_h channels at an incidence angle of 53° . Besides the brightness temperatures of two principal polarizations (T_v and T_h), traditionally used for earth remote sensing, **near-nadir** looking observations made by Dzura et al.¹⁰ at Ku-band (14 GHz) showed the sensitivity of the third Stokes parameter to wind direction. To explore the **polarimetric** brightness temperatures of sea surfaces at off-nadir incidence angles, the Jet Propulsion Laboratory has deployed a K-band (19.35 GHz) **multi-polarization** radiometer (WINDRAD)¹¹ on the NASA DC-8 aircraft with circle flights over several National Data Buoy Center (NDBC) buoys in November 1993. These measurements **demonstrated** that the first three Stokes parameters of sea surface emissions are sensitive to ocean wind directions in the incidence angle range of 30° to 50° . Subsequently, JPL added a 37-GHz channel to the WINDRAD and flew the dual-frequency system in 1994 over the NDBC buoys off the California coast to study the frequency sensitivities from 45° to 65° incidence angles'. Measured radiometric temperatures showed a few Kelvin azimuth modulations in all Stokes parameters with respect to the wind direction. Wind directional signals observed in the 37 GHz channel were similar to those in the 19 GHz channel, indicating a weak frequency dependence of the wind direction signals in sea surface brightness temperatures in the range of 19 to 37 GHz. Altogether these experimental data provided a **proof-of-concept demonstration** that polarimetric sea

surface brightness temperatures are influenced by the preferential directional forcing of surface winds in the range of incidence angles from 0° to 65°.

However, these data sets are insufficient for a more comprehensive assessment of the wind speed and incidence angle sensitivities of wind direction signals. To fully explore the wind direction signals in passive brightness temperatures over a large range of wind speeds, the JPL WINDRAD was deployed on NASA DC-8 in 1995 and on NASA Wallops P-3 aircraft in 1996 to acquire additional data at low and high winds.

5.2 JPL Polarimetric Radiometer Experiments

Electromagnetic waves emitted from natural media due to random thermal motion of electric charges are in general partially polarized¹². To fully characterize the polarization state of a partially polarized thermal radiation, four parameters **1, Q, U, and V** were introduced by Sir George Stokes¹³. Because conventional radiometers for earth remote sensing measure T_v and T_h , an alternate representation is to use a modified form of Stokes vector with four parameters, T_v , T_h , U , and V :

$$I_s = \begin{bmatrix} T_v \\ T_h \\ U \\ V \end{bmatrix} = c \begin{bmatrix} \langle |E_v|^2 \rangle \\ \langle |E_h|^2 \rangle \\ 2\text{Re}(E_v E_h^*) \\ 2\text{Im}(E_v E_h^*) \end{bmatrix} = \begin{bmatrix} T_v \\ T_h \\ T_p - T_m \\ T_L - T_R \end{bmatrix}$$

T_v and T_h are the brightness temperatures of vertical and horizontal polarizations, while U and V characterize the correlation between these two orthogonal polarizations. Note that $T_v + T_h$ represents the total radiated energy, and $Q = T_v - T_h$ the polarization difference. The second equality relates Stokes parameters to the horizontally and vertically polarized components of electric fields (E_h and E_v). The angular brackets denote the ensemble average of the argument, and c is a proportionality constant relating the brightness temperature to the electric energy density. The last equality shows that the third and fourth Stokes parameters can be related to the brightness temperatures measured at 45°-linear (T_p), -45°-linear (T_m), left-hand circular (T_L), and right-hand circular (T_R) polarizations.

To acquire polarimetric ocean brightness temperatures, a dual-frequency polarimetric radiometer system operating at 19 GHz (K band) and 37 GHz (Ka band) was built by the Jet Propulsion Laboratory in 1993 and 1994. A more detailed description of the dual-frequency radiometer system can be found in Refs. 4 and 11. The dual-frequency radiometer system was deployed on the NASA DC-8 in 1994 and 1995 and on the NASA P-3 in 1996 over a large range of wind speeds over the National Data Buoy Center (NDBC) moored buoys, which provided ocean wind speed and direction measurements.

The radiometer antennas were mounted on the aircraft windows at an angle of 75° from nadir. To obtain data at the desired incidence angles of 45°, 55° and 65°, the aircraft was banked at 30°, 20°, and 10°, respectively. At each bank angle, the aircraft performed circle flights, enabling the acquisition of radiometers data from all azimuth angles with respect to the surface wind direction.

The key results from the flight experiments are as follows:

1. There are wind direction signals at 2-24 m/s wind speeds in the polarimetric U channel,
2. T_v , T_h and Q also exhibit wind direction signals over clear skies, but are sensitive to clouds. In the presence of cloud cover, the directional signals in T_v and T_h are masked by the microwave radiation from clouds. $Q = T_v - T_h$ appears to be less sensitive to clouds than T_v and T_h .

3. **There** are cases that the cloud radiation along the radiometer to surface path is canceled in Q , but frequently the reflected downwelling cloud radiation could not be removed by taking the difference of T , and T_h .
4. The signals increase with increasing wind speed, except the upwind and crosswind asymmetry of U at 65° incidence angle showing a stronger than expected magnitude.
5. The signals are small at low winds ($<5\text{ m/s}$), **in particular at 55 degree incidence angle**. This implies that a spaceborne radiometer requires a sensitivity of 0.1 Kelvin or better to perform wind direction measurements at low **winds, In addition, the data show that 550 incidence angle might not be suitable for low wind measurements from space. For moderate wind speeds ($5\text{-}10\text{ m/s}$), the directional signals are stronger at lower incidence angles.**
6. There is a stronger upwind and downwind asymmetry at higher angles. This suggests that a radiometer operating at 65° incidence **angle will have a better skill than those operating at lower incidence angles.**
7. The wind direction signals are similar at 19 and 37 GHz. However, the signals at 37 GHz are slightly stronger than those from 19 GHz channel.
8. Limited high wind data from flights near Hurricane **Juliette** indicate that there is a strong directional signal in U at 450 incidence angle at 24 m/s .

5.3 WINDRAD Experiment on SeaWinds-1 B

The experimental observations mentioned above suggest a strong potential of passive microwave radiometry for large spatial coverage of ocean surface wind vector measurements. However, several outstanding issues must be investigated before such a technique is utilized **for large scale observations**. Namely:

1. Can passive radiometers perform wind direction measurements over a large **range** of atmospheric and oceanic conditions? ERS-1 **1-2 scatterometers** and NSCAT have demonstrated reasonable directional accuracy over cyclones and low wind areas, but it is also known that **scatterometer measurements** can be affected by long surface waves and sea surface and air temperatures. It is important to know whether passive microwave radiometers can provide comparable performance over the same range of wind speeds and also whether the other oceanic parameters have significant effects.
2. **What is the influence of the atmosphere on radiometer wind vector measurements? Passive microwave radiometric signals are sensitive to atmospheric liquid water and water vapor. The atmospheric radiation and attenuation, if not properly removed, will be confused as the emission from the sea surface and contaminate the wind direction signals. Since about 50 percent of the earth is covered by clouds at any time, it is imperative to quantify the effects of clouds on all polarization channels.**
3. What are the appropriate measurement **geometry** and requirements for spaceborne radiometers? Key **parameters** for a spaceborne instrument include the incidence angle(s), frequencies, scanning configurations (1 look vs. 2 looks), polarizations, and radiometer sensitivity.

The data from SeaWinds/WINDRAD experiment will permit the validation of spaceborne WINDRAD accuracy and a direct comparison of scatterometer and radiometer techniques.

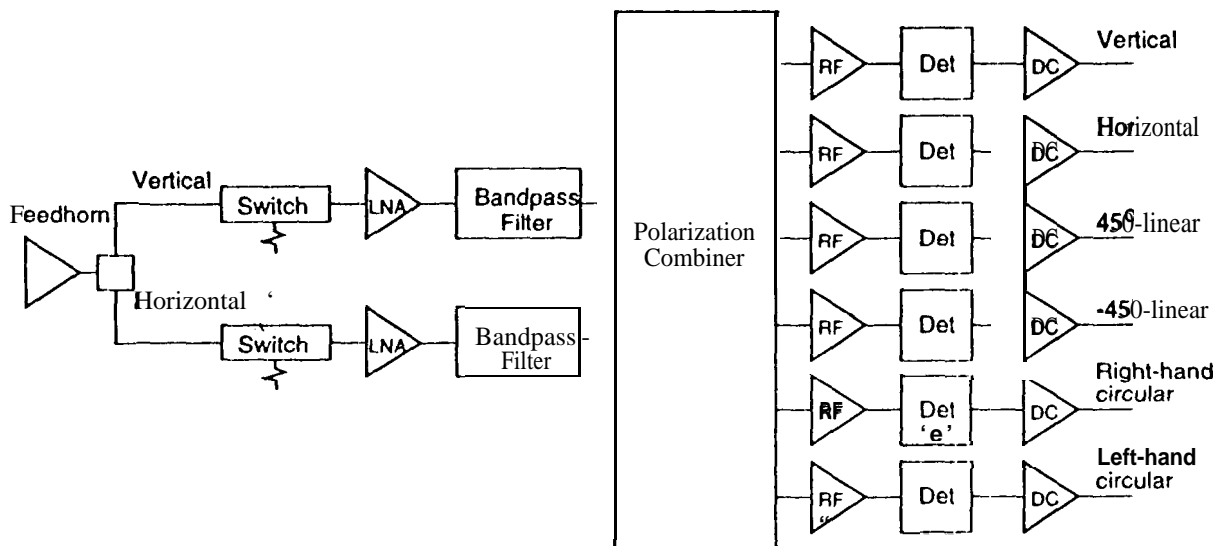
5.4 Spaceborne WINDRAD System Design

The WINDRAD on SeaWinds-1 B will share the reflector antenna with the scatterometer. Three multi-frequency feedhorns will be used to illuminate the reflector, producing three antenna beams at 45° , 53° , and 65° incidence angles. Table 1 summarizes the key parameters of the WINDRAD on SeaWinds-1 B. The radiometer will operate at two of the three incidence angles simultaneously, resulting in four azimuth looks for the overlapping portion of swaths. Three frequencies are used for each incidence angle. 18 and 37 GHz

channels are **fully polarimetric** and will provide the wind speed and direction measurements, **while 22 GHz channel will provide data for atmospheric water vapor correction.**

A functional **block diagram for the WINDRAD system is shown in Figure 5.** Each feedhorn provides the **vertically and horizontally electric fields (E_v and E_h) for each frequency through the waveguides to the WINDRAD Electronic Subsystem for power detection.** For 18 GHz and 37 GHz channels, E_v and E_h are **then amplified by two low noise amplifiers and fed through a polarization combiner to produce 450-linearly, -450-linearly, left-hand circularly, and right-hand circularly polarized electric fields in addition to vertical and horizontal polarizations.** The six **channel outputs from the polarization combiner are power-detected and sampled simultaneously.** The sampled signals are sent through the slip ring to CDS for telemetry packaging and downlink. (The 22-GHz channels will not have the polarization combiner and will **only output vertically and horizontally polarized power measurements.**) The use of the polarization combiner is to enable a **simultaneous measurement of T_v, T_h, T_p, T_m, T_L and T_R to achieve the radiometer sensitivity of about 0.1 Kelvin.**

Figure 5. WINDRAD System Functional Block Diagram



The radiometer receiver will be calibrated by *noise diodes* and reference loads at the outer edges of antenna scanning circles. The equivalent noise temperature of noise diodes will be calibrated during system integration and calibration tests. Thermistors attached on the *referenceloads* and the waveguides from the feedhorns to the electronics subsystem will provide physical temperatures of these components, which will be included as part of the telemetry for brightness temperature calibration

The WINDRAD ground data processing consists of two steps to reduce spacecraft telemetry into geophysical parameters. First, the instrument telemetry and spacecraft ephemeris are used to produce **earth-located** brightness temperatures. Next, the geophysical processing retrieves the geophysical parameters, including wind speed and direction along with atmospheric parameters from collocated brightness temperatures acquired at multiple azimuth looks. Processing will be performed for a range of incidence angle, azimuth angle, and frequency combinations. This will enable us to address the issues posed in the previous section.

REFERENCES

1. L. Grantham, E. M. Bracalente, W. Linwood Jones, and J. W. Johnson, "The SeaSat-A Satellite Scatterometer", *IEEE J. Oceanic Eng.*, OE-2, pp200-206, 1977
2. F. M. Nader¹, M. H. Freilich, and D. G. Long, "Spaceborne Radar Measurement of Wind Velocity Over the Ocean - An Overview of the NSCAT Scatterometer System", *Proc. IEEE*, Vol. 79, No. 6, pp 850-866, 1991
3. C. Wu, J. Graf, M. Freilich, D. G. Long, M. Spencer, W. Tsai, D. Lisman, and C. Winn, "The SeaWinds scatterometer instrument", *Proc. Int. Geosci. Remote Sensing Symp.*, Pasadena, CA, August 8-12, pp1511-1515, 1994
4. S. H. Yueh, W. J. Wilson, F. K. Li, W. B. Ricketts, and S. V. Nghiem, "Polarimetric brightness temperatures of sea surfaces measured with aircraft K- and K-band radiometers," *IEEE Trans. Geosci. Remote Sensing*, Vol. 35, No. 5, 1997.
5. Evert P. W. Attema, "The Active Microwave Instrument On-Board the ERS- 1 Satellite", *Proc. IEEE*, vol. 79, NO.6, pp79 1-799, 1991
6. J. P. Hollinger, J. L. Peirce, and G. A. Poe, "SSM/I instrument evaluation," *IEEE Trans. Geosci. Remote Sensing*, Vol. 28, No. 5, pp78 I-790, Sep., 1990.
7. V. S. Etkin, M. D. Raev, M. G. Bulatov, Yu. A. Militsky, A. V. Smimov, V. Yu. Raizer, Yu. A. Trokhimovsky, V. G. Irisov, A. V. Kuzmin, K. Ts. Litovchenko, E. A. Bepalova, E. I. Skvortsov, M. N. Pospelov, and A. I. Smimov, *Radiohydrophysical Aerospace Research of Ocean, Report II p1749*, Academy of Sciences, Space Research Institute, Moscow, USSR, 1991.
8. V. G. Irisov, A. V. Kuzmin, M. N. Pospelov, J. G. Trokhimovsky, and V. S. Etkin, "The dependence of sea brightness temperature on surface wind direction and speed. Theory and Experiment," *IEEE, Proceedings of International Geoscience and Remote Sensing Symposium*, Houston, 1992.
9. F. J. Wentz, "Measurement of oceanic wind vector using satellite microwave radiometers", *IEEE Trans. Geosci. Remote Sensing*, Vol. 30, No. 5, pp960-972, Sep., 1992.
10. M. S. Dzura, V. S. Etkin, A. S. Khrupin, M. N. Pospelov, and M. D. Raev, "Radiometers-polarimeters: principles of design and applications for sea surface microwave emission polarimetry," *Proceedings of International Geoscience and Remote Sensing Symposium*, Houston, 1992.
11. S. H. Yueh, W. J. Wilson, F. K. Li, W. B. Ricketts, and S. V. Nghiem, "Polarimetric measurements of sea surface brightness temperatures using an aircraft K-band radiometer," *IEEE Trans. Geosci. Remote Sensing*, Vol. 33, No. 1, pp85-92, 1995.
12. John D. Kraus, *Radio Astronomy*, 2nd. cd., 1986, Cygnus-Quasar Books, Powell, Ohio.